ADVANCED FUNCTIONAL MATERIALS
www.afm-journal.de

Multi-Site Functionalization of Protein Scaffolds for Bimetallic Nanoparticle Templating

*Kelly N. L. Huggins, Alia P. Schoen, Manickam Adhimoolam Arunagirinathan, and Sarah C. Heilshorn**

The use of biological scaffolds to template inorganic material offers a strategy to synthesize precise composite nanostructures of different sizes and shapes. Proteins are unique biological scaffolds that consist of multiple binding regions or epitope sites that site-specifically associate with conserved amino acid sequences within protein-binding partners. These binding regions can be exploited as synthesis sites for multiple inorganic species within the same protein scaffold, resulting in bimetallic inorganic nanostructures. This strategy is demonstrated with the scaffold protein clathrin, which self-assembles into spherical cages. Specifically, tether peptides that noncovalently associate with distinct clathrin epitope sites, while initiating simultaneous synthesis of two inorganic species within the assembled clathrin protein cage, are designed. The flexibility and diversity of this unique biotemplating strategy is demonstrated by synthesizing two types of composite structures (silver–gold mixed bimetallic and silver–gold core–shell nanostructures) from a single clathrin template. This noncovalent, Template Engineering Through Epitope Recognition, or TEThER, strategy can be readily applied to any protein system with known epitope sites to template a variety of bimetallic structures without the need for chemical or genetic mutations.

1. Introduction

Biotemplating, the synthesis of inorganic material using biological materials as scaffolds, has been successfully achieved using a wide variety of templates including viruses, bacteria, DNA, lipids, and peptide and protein assemblies.[1–9] These biotemplates continue to be attractive scaffolds because of their nanoscale dimensions, structural diversity, and potential inorganic specificity, resulting in the controlled synthesis of nanoscale inorganic material. While several elegant methods have been developed to template specific inorganic nanoparticles for the design of functional materials, the ability to interface with multiple inorganic species simultaneously, in a controlled manner, remains an ongoing area of research.[10–16] Here, we demonstrate that our unique biotemplating strategy can achieve concurrent inorganic templating within a single scaffold, the clathrin protein, exploiting its multiple epitope regions as synthesis sites.

Clathrin is an intracellular protein that plays a major role in the formation of coated vesicles to transport cargo within cells. A single clathrin triskelion unit is made of three semi-flexible arms (**Figure 1**a) that self assemble within cells to form both 2D lattices (at the lipid membrane) and 3D structures (around lipid vesicles) (Figure 1a). Outside of the cellular environment, purified clathrin assembles to form multiple nano-architectures including spheres, barrels, tetrahedra, and cubes, depending on the environmental conditions (e.g., pH, concentration, buffer ionic strength).[17–20] This structural diversity exhibited by a single scaffold makes clathrin an ideal protein model for templating inorganic materials.

Clathrin also contains multiple epitope sites (i.e., binding pockets) that facilitate interactions with clathrin-adaptor-proteins, which initiate clathrin self-assembly as well as trigger endocytosis and cargo transport across the cell membrane.[21,22] Previously, we reported that one of these epitope sites, the C-box, could be functionalized to facilitate the synthesis of inorganic material within the assembled clathrin protein cage.[23] This unique templating strategy, Template Engineering Through Epitope Recognition, or TEThER, mimics adaptor-protein interactions by using engineered tether peptides that noncovalently bind to the clathrin protein, while exposing an inorganic binding sequence designed to initiate inorganic synthesis (Figure 1b,c). Unlike existing methods of biotemplating with viral cages, bacteria, or other proteins, the TEThER strategy offers a unique way to template specific inorganic nanomaterial without genetic or chemical modifications to the scaffold. This strategy therefore, creates a versatile, mix-and-match method to synthesize a range of nanoparticle sizes, shapes, and compositions that can be applied to any protein scaffold.

Our first account of this technique utilized a single epitope site to synthesize a single metal or metal oxide species at a time

K. N. L. Huggins, A. P. Schoen, M. A. Arunagirinathan, Prof. S. C. Heilshorn
Materials Science & Engineering
476 Lomita Mall
Stanford University
Stanford, CA 94305, USA
E-mail: heilshorn@stanford.edu
K. N. L. Huggins, A. P. Schoen, M. A. Arunagirinathan, Prof. S. C. Heilshorn
Stanford Institute for Materials and Energy Science
SLAC National Accelerator Laboratory
Menlo Park, CA 94025, USA

DOI: 10.1002/adfm.201402049

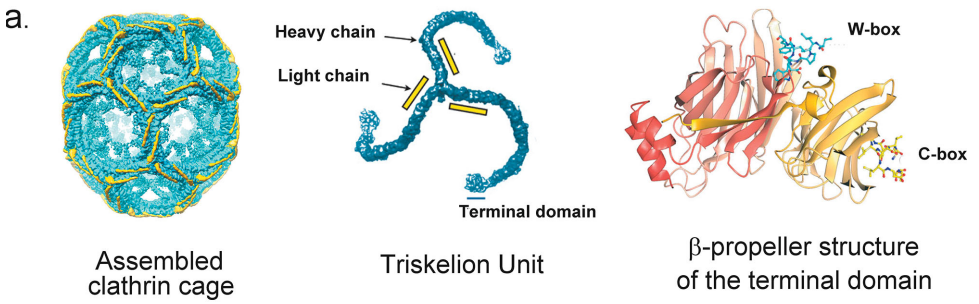

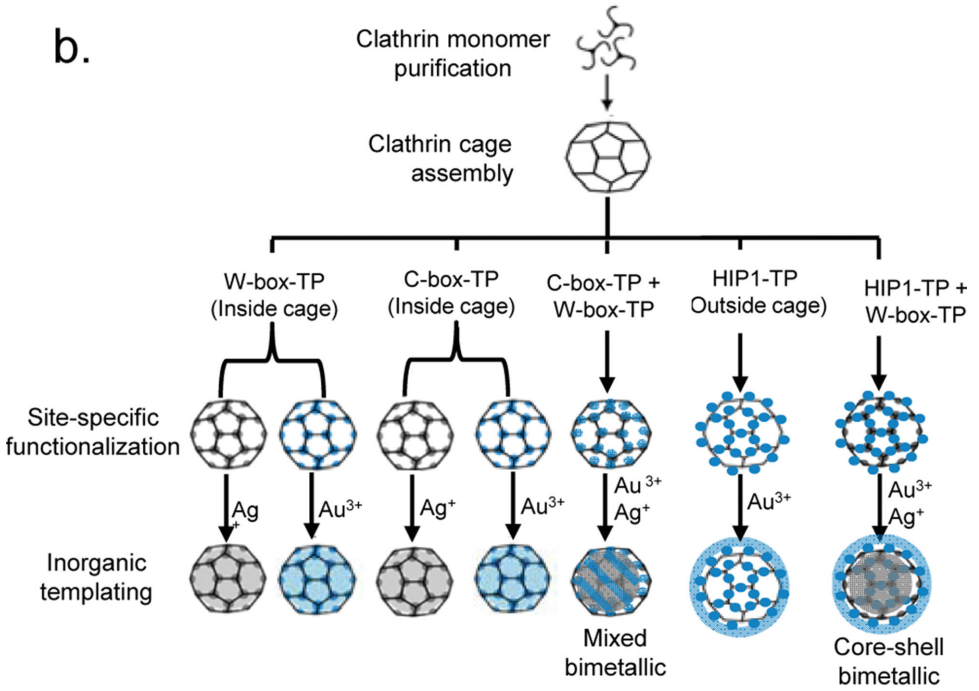

c.

clathrin binding — linker — inorganic binding

TEThER Peptide (TP)	Sequence
C-box-Au	KDVS**LLDLD**DFN---GGGG---AHHAHHAAD
C-box-Ag	KDVS**LLDLD**DFN---GGGG---NPSSLFRYLPSD
W-box-Au	TL**PWDLW**TT---GGGG---AHHAHHAAD
W-box-Ag	TL**PWDLW**TT---GGGG---NPSSLFRYLPSD
HIP1-Au	GSHA**DLLR**KNAEVTKQ---GGGG---AHHAHHAAD

Figure 1. a) Representative structure of an assembled 50 nm clathrin cage (left panel) and a single triskelion unit (middle panel) showing the location of the light chains (yellow) and heavy chains (blue). Ribbon representation (right panel) of the clathrin *β*-propeller terminal domain and stick models of the clathrin-binding C-box and W-box peptides. Images reprinted by permission from Macmillan Publishers Ltd: Nature, Nature Structure and Molecular Biology, copyright 2004.[27,29] b) Schematic of the TEThER biotemplating process. Clathrin monomers are assembled into cage structures and chemically fixed. The TEThER peptides (TPs) are added to noncovalently functionalize the inside and/or outside of the clathrin cage. Gold or silver precursor molecules are added to initiate templating in solution at room temperature and pressure. c) Amino acid sequences of the TPs used in this study. Sequences underlined and bolded correspond to the minimally active, clathrin-binding portion of the peptide sequence. Sequences in blue or gray represent inorganic-binding regions for gold and silver, respectively.

Adv. Funct. Mater. **2014**,
DOI: 10.1002/adfm.201402049

within the clathrin cage.[23] The purpose of the current work is to expand the versatility and utility of the TEThER strategy by introducing two new epitope sites for inorganic templating, one on the inside and one of the outside of the assembled clathrin cage. We demonstrate that these epitope sites can be used simultaneously to mediate interactions with multiple inorganic species to synthesize bimetallic nanostructures.

Bimetallic composite structures have enhanced catalytic and optical properties compared to single-component materials, and the control over their size, shape, and composition is critical to material function.[15,16,24] We use the TEThER strategy to synthesize two types of silver–gold composite structures, a mixed bimetallic and a defined core–shell nanostructure, by noncovalent site-specific interactions with the self-assembled, clathrin protein scaffolds. This work shows TEThER to be a versatile method that can be extended to synthesize composite materials, making it an attractive strategy for inorganic biotemplating.

2. Results and Discussion

Purified clathrin monomers were reassembled in vitro into spherical cage structures with an average diameter of 50 nm and subsequently covalently crosslinked with paraformaldehyde to prevent disassembly during the templating reactions.[20,25] Using our TEThER biotemplating method, the fixed clathrin cages were then functionalized with engineered peptides designed to enable site-specific interactions with metallic ions. In our previous work, we utilized the C-box epitope site, which is located on the N-terminal domain of the clathrin foot (Figure 1a), to design a TEThER peptide (TP) consisting of a C-box sequence, a tetraglycine linker for conformational flexibility, and an inorganic recognition sequence (Figure 1c).[23,26]

We now extend the TEThER method to include multiple recognition sites within clathrin to achieve simultaneous localization of two different inorganic ions at distinct sites within a single protein scaffold. Two new TP clathrin-binding domains were designed to functionalize the clathrin scaffold at two additional epitope sites: the W-box and the Huntingtin Interacting Protein (HIP1) binding sites (Figure 1). The W-box TP domain is a tryptophan-containing peptide sequence, PWDLW, that was designed based on a specific region of the human amphiphysin I protein that associates with clathrin in vivo.[27,28] Crystallographic structural and binding studies revealed that expanding the minimally active W-box sequence to include the two flanking residues on either side resulted in relatively strong peptide-clathrin association and thus were included in our studies (Figure 1c).[27]

The W-box-TP domain, like the C-box-TP domain, is designed to specifically bind to the N-terminal domain of the clathrin foot, which positions the peptides on the inside of the assembled cage.[27,30] In contrast, the HIP1-TP domain is designed to bind to the HIP1 site located on the clathrin light chain near the vertex of the triskelion unit; therefore, once the clathrin monomers are assembled, the HIP1-TP domain is situated on the outside of the clathrin cage (Figure 1).[31] We designed the HIP1-TP domain based on early mutagenesis studies and crystallographic data that identified the DLLRKN peptide sequence as a critical site of interaction between the HIP1 helical domain and the clathrin light chain.[22,32] We incorporated additional flanking residues that have been shown to play a role in HIP1-clathrin association.[22]

Like the C-box-TP design, both the W-box-TP and HIP1-TP contain inorganic binding sequences linked to the clathrin-binding domain through a tetraglycine linker (GGGG). This combinatorial peptide strategy was used to design peptides for gold and silver synthesis at W-box epitopes (W-box-Au and W-box-Ag, respectively) and gold synthesis at the HIP1 epitope sites (HIP1-Au) (Figure 1c). For proof of concept experiments, we selected inorganic binding sequences previously reported to synthesize gold and silver nanoparticles.[33,34]

2.1. W-box-Au-TP Nucleation of Gold Nanoparticles

To initiate the gold templating reaction at the W-box site, a gold inorganic precursor ($HAuCl_4$) was added to a sample consisting of assembled clathrin cages pre-incubated with W-box-Au-TP. After overnight incubation in the dark, transmission electron microscopy (TEM) and energy dispersive X-ray spectroscopy (EDS) analysis revealed gold particles with an average diameter of 6.4 ± 4.8 nm (**Figure 2**).

As previously reported, control reactions consisting only of assembled clathrin cages (i.e., no TPs) were able to nonspecifically reduce the gold precursor, resulting in large, irregular clusters of gold nanoparticles (Figure S1, Supporting Information). This is presumably due to nonspecific nucleation of gold by charged amino acid residues on the clathrin surface.[35] We have previously reported that the C-box-Au-TP acts both as a nucleating agent to concentrate soluble gold ions within the cage and as a capping agent to limit the growth and agglomeration of the nanoparticles.[23,33] It is likely the W-box-Au-TP also serves these dual roles in gold nanoparticle synthesis.

Consistent with this hypothesis, W-box-Au-TP incubated with gold precursor without cages resulted in the formation of a few small, irregular gold particles (Figure S1, Supporting Information) that were inconsistent in shape and size. This confirms that the W-box-Au-TP must be concentrated within the clathrin cage to be effective. Gold precursor in the absence of clathrin and TPs resulted in a few irregular gold nanoparticles that were much larger in size, as predicted in the absence of peptide capping agents (Figure S1, Supporting Information). These results are expected, as the gold precursor used in our study is quite reactive.[35–37] These data illustrate that similar to the C-box-Au-TP, the W-box-Au-TP acts both as a tether and a capping agent within the clathrin cage to achieve regulation of gold nanoparticle size and shape.

2.2. W-box-Ag-TP Nucleation of Silver Nanoparticles

In our previous work we demonstrated gold, titanium dioxide, and cobalt oxide synthesis using the C-box epitope as the binding site. In this study we demonstrate further the versatility of the TEThER system by synthesizing silver nanoparticles at both the W-box and C-box sites. In the presence of a silver precursor, $AgNO_3$, and assembled clathrin cages, W-box-Ag-TP initiated the synthesis of spherical silver nanoparticles with

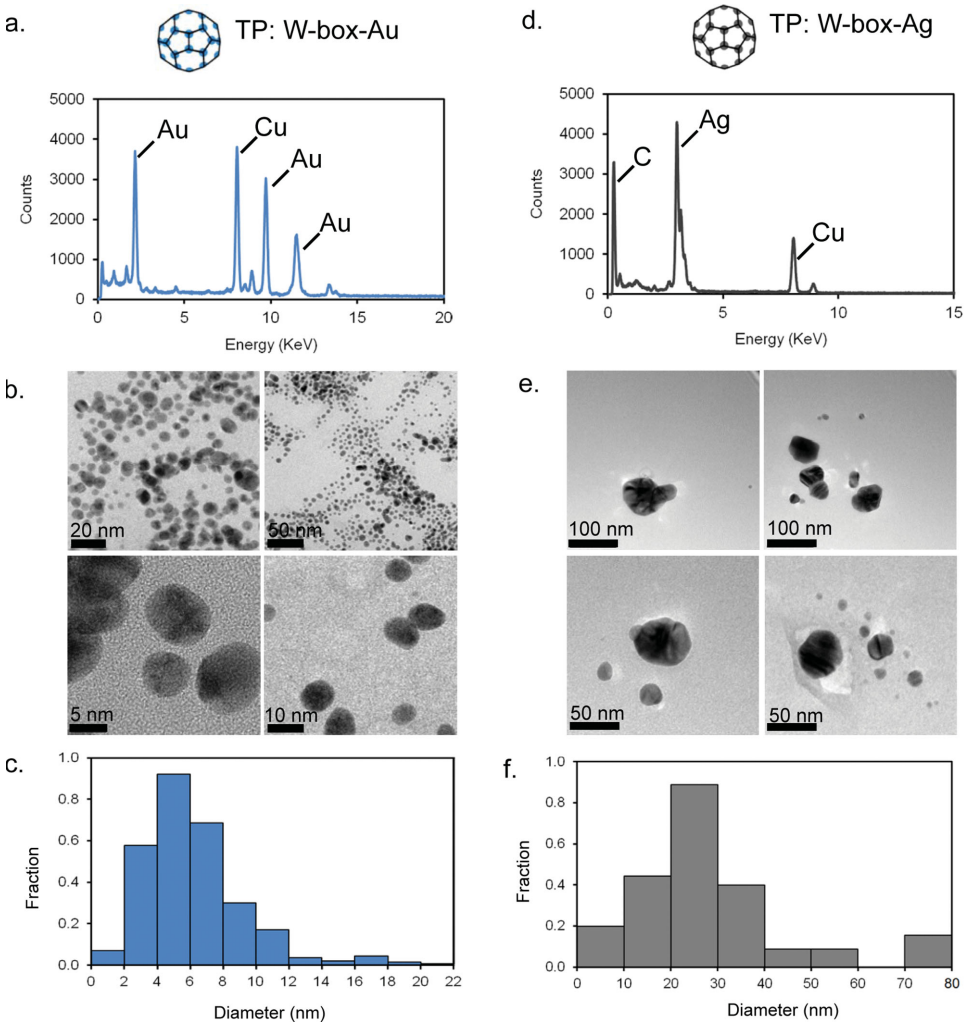

Figure 2. W-box-TP mediated templating reactions for a–c) gold and d–f) silver. A schematic of the templating reactions are shown above each EDS panel. a,e) EDS data confirming the presence of gold or silver, respectively; the copper (Cu) peaks are a result of the small non-collimated signal of the beam interacting with the large volume of the Cu grid. b,e) TEM analysis of particles formed in the presence of clathrin cages and W-box-Au-TP plus gold precursor or W-box-Ag-TP plus silver precursor, respectively. c,f) Histograms illustrating diameter distribution of templated gold or silver nanoparticles.

an average diameter of 28.8 ± 18 nm (Figure 2). As a control, clathrin cages in the presence of silver precursor without TPs formed large, flower-like, silver nanoparticles (Figure S2, Supporting Information). Similar to the W-box-Au-TP mediated gold templating reaction, these data confirm that although charged amino acid residues on the clathrin cage surface are sufficient to initiate silver nucleation, the presence of the designed TP is required to control particle size and shape. The silver precursor in the absence of peptide and assembled clathrin cages resulted in large silver particle aggregates, suggesting that the W-box-Ag-TP may also be acting as a capping agent to prevent agglomeration (Figure S2, Supporting Information).

To demonstrate the requirement for epitope site-specificity of W-box domain TPs, we designed a non-binding peptide control, W-box-Ctrl-Ag-TP, that consisted of alanine substitutions at sites critical for peptide-clathrin interaction (Figure S3, Supporting Information). W-box-Ctrl-Ag-TP in the presence of the assembled clathrin cage and silver precursor resulted in particles ranging in size from 40 nm to >200 nm (average 112.6 nm ± 46.2 nm, Figure S3, Supporting Information). This broad size distribution suggests that without site-specific interaction between the peptide and clathrin cage, controlled synthesis cannot be achieved.

2.3. Bimetallic Nanoparticle Synthesis using the W-box and C-box Epitope Sites

In the presence of assembled clathrin cages, C-box-Ag-TP, and silver precursor; small, spherical silver nanoparticles ($d = 48.5 \pm 33.5$ nm) were formed, similar to those synthesized in the presence of clathrin decorated with W-box-Ag-TP (**Figure 3**a,b). The use of a C-box non-binding peptide control (C-box-Ctrl-Ag-TP) resulted in much larger silver nanoparticles ($d = 136 \pm 58.6$ nm) with a broad size distribution (Figure S3, Supporting Information). These results were similar to the W-box-Ctrl-Ag-TP reactions and again illustrate the limited control over growth when the TP is not localized within the clathrin cage.

Adv. Funct. Mater. **2014**,
DOI: 10.1002/adfm.201402049

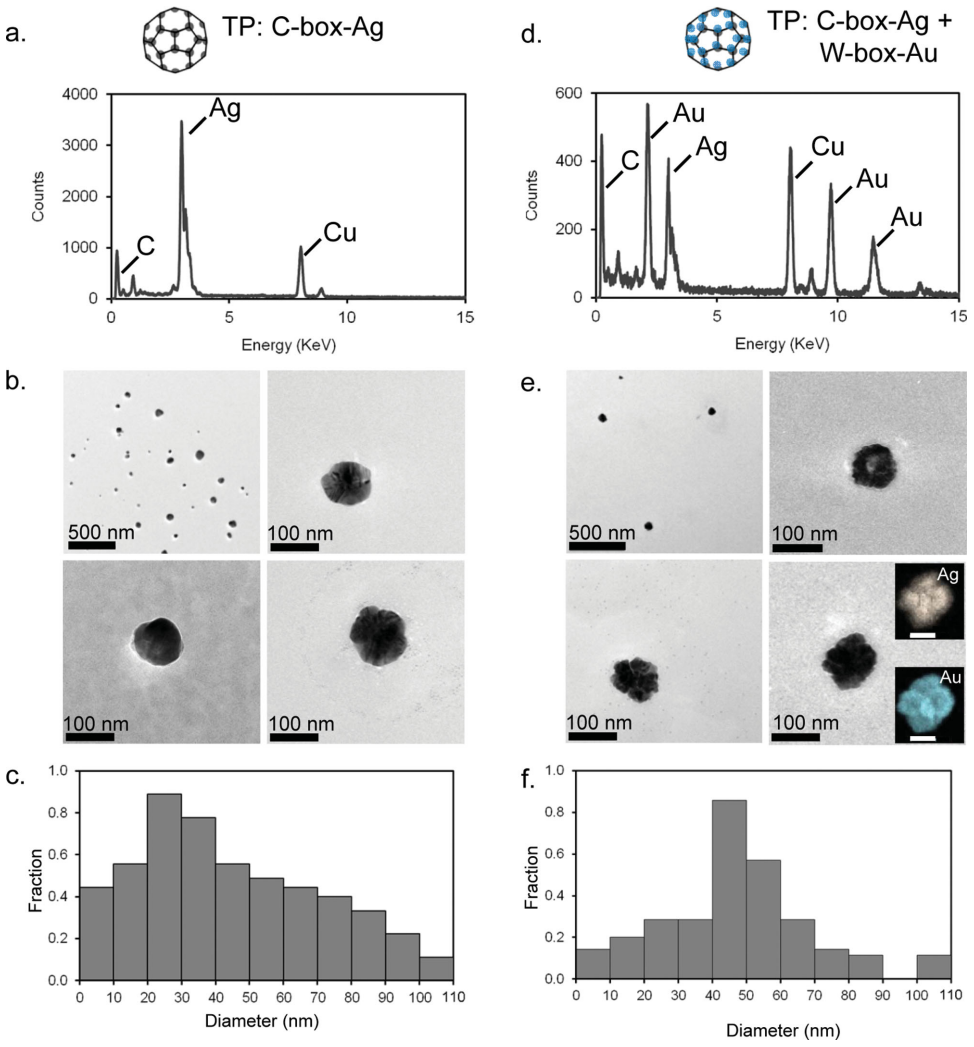

Figure 3. a–c) C-box-Ag-TP mediated silver templating reactions and d–f) mixed bimetallic gold-silver templating. A schematic of the templating reactions are shown above each TEM panel. a,b) EDS and TEM analysis of particles formed in the presence of C-box-Ag-TP, silver precursor, and clathrin cages. c) Histogram of diameter distribution for templated gold nanoparticles. d,e) EDS and TEM analysis of particles formed in the presence of C-box-Ag-TP, W-box-Au-TP, mixed precursors (i.e., $HAuCl_4$ and $AgNO_3$), and clathrin cages. EDS mapping illustrates silver and gold within the same particle (panel (e), bottom right image insets, scale bar = 50 nm). f) Histogram of diameter distribution for mixed bimetallic silver–gold templated particles.

Both the W-box and C-box sites, which are located on the inside of the assembled clathrin cage, can function as nucleation sites for the synthesis of either silver or gold nanoparticles. Therefore, to extend the versatility of our TEThER strategy, we next tested if both the W-box and C-box sites could be used simultaneously to synthesize composite gold-silver nanostructures inside the assembled clathrin cage. The bimetallic templating reactions were carried out by simultaneous addition of gold and silver precursors ($HAuCl_4$ and $AgNO_3$, respectively) to a solution of clathrin cages with the W-box-Au-TP and C-box-Ag-TP peptides. This reaction resulted in nanoparticles with an average diameter of 41.3 ± 24.0 nm, consistent with the size of an assembled clathrin cage (≈50 nm) (Figure 3f). These nanoparticles were analyzed by EDS, which confirmed the presence of gold and silver within each particle (Figure 3d). A scanning TEM (STEM) EDS mapping analysis revealed that both gold and silver were distributed throughout the entire mixed bimetallic structure (Figure 3e insets). Because both sites are located on the N-terminal domain and are in close proximity to each other (within 25 Å), it is difficult to correlate the material distribution to the location of the epitope site. However this initial experiment indicates that our templating method is effective at synthesizing bimetallic composite structures within the protein cage scaffold.

Control reactions that consisted of only clathrin cages in the presence of mixed precursors (i.e., $HAuCl_4$ and $AgNO_3$) resulted in a few, irregularly shaped gold nanoparticles with no significant traces of silver (Figure S4, Supporting Information). Similarly, reactions that consisted of only mixed precursors in the presence of TPs (i.e., without clathrin cages) formed only gold nanoparticles (Figure S4, Supporting Information). These control data further confirm that the formation of bimetallic composite structures requires the presence of clathrin cages and both engineered TPs.

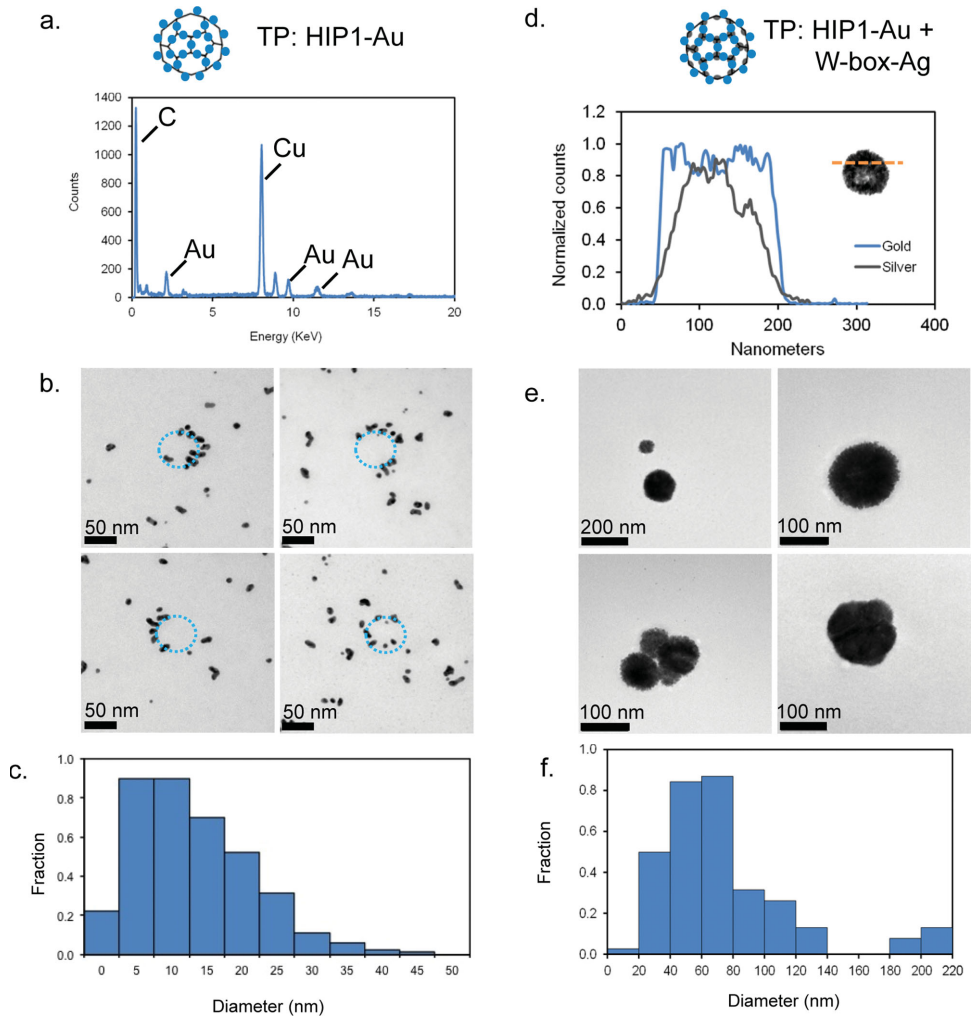

Figure 4. a–c) HIP1-Au-TP mediated gold and d–f) core–shell silver–gold composite reactions. A schematic of the templating reactions are shown above each EDS panel. a,b) EDS and TEM analysis of particles formed in the presence of HIP1-Au-TP, gold precursor, and clathrin cages. c) Histogram of diameter distribution for templated gold nanoparticles. d) EDS analysis of composite core–shell nanoparticles formed in the presence of HIP1-Au-TP, W-box-Ag-TP, mixed precursor, and clathrin cages. Line scan STEM mapping shows the presence of a gold shell surrounding a silver core. e) TEM analysis and f) histogram of diameter distribution for composite core–shell silver–gold templated particles.

2.4. Core–Shell Nanoparticle Synthesis using the HIP1 and W-box Epitope Sites

We next examined whether the HIP1 epitope site, which is located on the outside of the assembled clathrin cage, could be successfully used with the TEThER strategy to synthesize nanoparticles. In the presence of gold precursor and clathrin cages, HIP1-Au-TP mediated the synthesis of small gold nanoparticles with an average diameter of 17.6 ± 5.6 nm (**Figure 4**). As in our previous work, a fraction of the gold nanoparticles in these reactions was found to dissociate from the clathrin cage to form discrete, single particles.[36] Interestingly, TEM analysis suggests that another fraction of the gold particles cluster to form a circular pattern with an estimated diameter of 50 nm, a size that is similar to the dimensions of an assembled clathrin cage (Figure 4b). The presence of multiple gold nanoparticles surrounding the protein cage, rather than a continuous coating of a gold shell, suggests that multiple, discrete gold nucleation events occurred on the outside of the clathrin template. This morphology of multiple, discrete particles is similar to that observed in other gold biotemplating reactions.[10,36] These data are consistent with our hypothesis that HIP1-Au-TP initiates the synthesis of gold nanoparticles on the outside of the assembled clathrin cage. No similar patterns were observed in any of the control samples for this templating reaction (Figure S5, Supporting Information).

We further hypothesized that by simultaneously utilizing the epitope sites located on the outside (HIP1) and inside (W-box) of the clathrin cage, our TEThER strategy could be used to design core–shell bimetallic nanoparticles. core–shell reactions were initiated by simultaneous addition of silver and gold precursors to a solution of W-box-Ag-TP, HIP1-Au-TP, and clathrin cages followed by incubation overnight. TEM analysis showed spherical particles with an average diameter of 64.9 nm ± 44.2 nm (Figure 4e,f). EDS analysis confirmed the presence of gold and silver (Figure S6, Supporting Information) for particles ranging

DOI: 10.1002/adfm.201402049

in size from 30–60 nm. The smaller particles (2–20 nm) included in the size distribution shown in Figure 4f consist of non-core–shell structures, i.e., nanoparticles consisting of gold or silver only, which result from unbound peptides in solution. As demonstrated in the control reactions, TEThER peptides free in solution without a clathrin template present will form this size range of nanoparticles (Figure S6, Supporting Information).

To further verify a core–shell distribution shown in Figure 4e, STEM EDS mapping was carried out at fixed points throughout a representative particle (Figure 4d and Supporting Information Figure S6). The graphical output generated from the STEM EDS mapping indicated both gold and silver signal intensity distribution. The gold shell is confirmed by enhanced gold signal present along the edges of the scan, while the silver core shows highest line scan intensity at the center of the particle, with little to no signal intensity at the edges of the particle.

The gold nanoparticles coat the cage more consistently than in the HIP1-Au-TP gold templating reaction (Figure 4b). This may be due to gold nanoparticles aggregating around the protein and exposed surface of the silver core. The gold shell is not limited by the size of the cage and therefore the gold nanoparticles continually nucleate and aggregate onto the surface of the cage and each other, resulting in core–shell nanoparticles that can exceed sizes of 100 nm.

Although not consistent for all silver particles, the silver core can also reach sizes up to 100 nm (Figure 4d–f). One proposed growth mechanism includes continuous coalescence of smaller silver particles in the presence of excess silver inorganic precursor.[39] This may cause the silver "core" to grow beyond the clathrin cage, forcing the protein scaffold to fall apart. We previously observed a similar phenomenon when using our TEThER strategy for the synthesis of titanium dioxide nanoparticles, whereby the TiO_2 nanoparticles grew beyond the size of the protein cage up to 200 nm in diameter.[23]

In addition, preformed gold nanoparticles attract silver ions onto their surface, catalyzing the reduction of Ag^+ to Ag^0. This may add further to the growth of the silver core and the favorable formation of the gold shell surrounding the silver nanoparticle.[11,40]

In control reactions, HIP1-Au-TP and W-box-Ag-TP without clathrin cages formed small gold particles with no presence of silver (Figure S6, Supporting Information). Together these data suggest that simultaneous TP binding to the HIP1 and W-box epitope sites results in the synthesis of silver–gold core–shell nanoparticles.

3. Conclusion

We have demonstrated that epitope-site recognition can be used as a noncovalent, mix-and-match method that synthesizes a variety of inorganic nanoparticles with control over composite inorganic material. In this study, the W-box and C-box sites were successfully used as nucleation sites for silver and/or gold synthesis within the assembled clathrin cage, while the HIP1 site, located on the surface of the clathrin cage, directed gold nucleation outside the clathrin cage scaffold.

Being able to control size, shape, and composition of bimetallic particles are consistent challenges faced in inorganic synthesis, as these characteristics govern the functionality of the material. We have designed a biomimetic method that can be carried out at room temperature and atmospheric pressure and in aqueous solvent environments to synthesize two types of composites, mixed bimetallic and core–shell. Our noncovalent templating method does not require chemical or genetic modifications of the protein scaffold to achieve site-specificity. As the repertoire of known peptide sequences that interact with inorganic materials continues to grow, this modular TP strategy could be used in a high-throughput fashion to synthesize a variety of nanoparticle composites. Similarly, while our proof of concept experiments utilized a clathrin scaffold, any self-assembling protein with known epitope sites should be amenable to the TEThER templating strategy.

4. Experimental Section

Clathrin Purification: As previously reported, clathrin protein was isolated from bovine brain tissue using centrifugation followed by column purification.[23,38] Briefly, frozen bovine brain tissue was obtained from VWR (Rockland ImmunoChemical) and blended with HKM buffer (25 mM HEPES, 125 mM potassium acetate, 5 mM magnesium acetate, 1 mM DTT, pH 7.4) at a concentration of 1 kg/L. After the tissue was homogenized, the suspension was centrifuged at 5,750 × *g* for 20 minutes and the resulting supernatant was collected and spun using an ultracentrifuge at 43 000*g* for 40 min. The pellets were then re-suspended in 30 mL of a 50/50 mixture of HKM and HKM plus 12.5 w/v % of Ficoll-sucrose. The suspension was subsequently sonicated for 1 min and centrifuged at 25 000*g* for 20 min. The supernatant was collected, combined with 3 volumes of HKM, and spun at 35 000*g* for 60 min. The resulting pellet, which consisted of clathrin-coated vesicles, was resuspended in approximately 2 mL of HKM and stored at –4 °C. To obtain clathrin monomers for the biotemplating reactions, the stored vesicles were re-suspended in dissociation buffer (1 M Tris, pH 7.0, 1 mM EDTA) and centrifuged at 22 000*g* for 20 min. The resulting supernatant was then loaded onto a Sepharose CL-4B gel filtration column, and fractions were analyzed by SDS-PAGE and Western blot (clathrin heavy chain monoclonal antibody X22, Calbiochem). Final products were analyzed by mass spectrometry (Stanford PAN Facility).

Clathrin Cage Assembly: Clathrin monomers were dialyzed into 2 mM Tris buffer, pH 7.0, and assembly was induced by adding 1/10 volume of 1 M MES, pH 6.0. Clathrin assembly was monitored by dynamic light scattering (DLS) over 20 min, after which samples were centrifuged at 16 000*g* for 10 min, decanted, then re-suspended with 100 mM MES, pH 6.0. To covalently fix the assembled clathrin cages, paraformaldehyde (PFA) was added to a final concentration of 4% and was allowed to react at room temperature for 15 min. The fixed samples were then centrifuged at 16 000*g* for 10 min, decanted, and suspended in approximately 20 µL of 100 mM potassium phosphate, pH 7.0, to dissociate any contaminating unfixed cages. Samples were then centrifuged at 16 000*g* for 10 min to isolate the fixed clathrin cages in the resulting pellet.

Biotemplating Reactions: Fixed clathrin cages were re-suspended in 100 mM potassium phosphate, pH 7.0, and incubated with 0.4–0.5 mg/mL final concentration of tether peptides for 15 min. All tether peptides were obtained from Genscript USA and dissolved in H_2O at a final stock solution of 4 mg/mL. For the gold templating reactions, the gold precursor $HAuCl_4$ was added to a final concentration of 2.7 mM. For silver reactions, the silver precursor $AgNO_3$ was added to a final concentration of 1 mM. Individual reactions were left to incubate in the dark overnight. For the simultaneous biotemplating of gold and silver, 10 µL of premixed precursor stock solution, consisting of 0.5 mM $AgNO_3$ and 1 mM $HAuCl_4$, was added to fixed cages plus C-box-Ag-TP and W-box-Au-TP or

fixed cages plus W-box-Ag-TP and HIP1-Au-TP. Reactions were incubated overnight in the dark. Control reactions omitting clathrin cages and/or tether peptides were run in parallel for all templating reactions.

TEM Preparation and Analysis: Carbon type-B support films on 400 mesh copper TEM grids (Ted Pella Inc.) were used to prepare samples for imaging. A 5-μL aliquot of each sample was placed onto the support film and allowed to dry. TEM was performed on an FEI Tecnai G2 F20 X-TWIN operated at 200 kV. Energy Dispersive X-ray Spectroscopy (EDS) elemental analysis and mapping were carried out using the TEM imaging and analysis (TIA) software. Particle diameters were quantified using manual tracing in Image J, and histograms were plotted in Excel.

Supporting Information

Supporting Information is available from the Wiley Online Library or from the author. It contains TEM and EDS analysis of control reaction products omitting required components of the templating reactions.

Acknowledgements

The authors thank Dr. Ai Leen Koh and Dr. Ann Marshall, Stanford Nanocharacterization Laboratory, for use of TEM facilities and helpful discussions and edits. A.P.S. acknowledges support from a Stanford Bio-X Fellowship and an Achievement Rewards for College Scientists Foundation (ARCS) Scholarship. This work is supported by the Department of Energy, Office of Basic Energy Sciences, Materials Sciences and Engineering Division, under contract DE-AC02-76SF00515.

Received: June 20, 2014
Revised: August 22, 2014
Published online:

[1] K. T. Nam, D.-W. Kim, P. J. Yoo, C.-Y. Chiang, N. Meethong, P. T. Hammond, Y.-M. Chiang, A. M. Belcher, *Science* **2006**, *312*, 885.
[2] B. Zhang, S. A. Davis, N. H. Mendelson, S. Mann, *Chem. Commun.* **2000**, *9*, 781.
[3] E. C. Samano, M. Pilo-Pais, S. Goldberg, B. N. Vogen, G. Finkelstein, T. LaBean, *Soft Matter* **2011**, *7*, 3240.
[4] S. L. Browning, J. Lodge, R. R. Price, J. Schelleng, P. E. Schoen, D. Zabetakis, *J. Appl. Phys.* **1998**, *84*, 6109.
[5] S. Lagziel-Simis, N. Coden-Hadar, H. Moscovich-Dagan, Y. Wine, A. Freeman, *Curr. Opin. Biotechnol.* **2006**, *17*, 569.
[6] J. M. Galloway, S. S. Staniland, *J. Mater. Chem.* **2012**, *22*, 12423.
[7] R. M. Kramer, C. Li, D. C. Carter, M. O. Stone, R. R. Nail, *J. Am. Chem. Soc.* **2004**, *126*, 13282.
[8] S. S. Behrens, *J. Mater. Chem.* **2008**, *18*, 3788.
[9] M. T. Klem, M. Young, T. Douglas, *J. Mater. Chem.* **2008**, *18*, 3821.
[10] Y. J. Lee, Y. Lee, D. Oh, T. Chen, G. Ceder, A. M. Belcher, *Nano Lett.* **2010**, *10*, 2433.
[11] T. Li, S. Chattopadhyay, T. Shibata, R. E. Cook, J. T. Miller, N. Suthiwangcharoen, S. Lee, R. E. Winans, B. Lee, *J. Mater. Sci.* **2012**, *22*, 14458.
[12] K. Govindaraju, S. K. Basha, V. G. Kumar, G. Singaravelu, *J. Mater. Sci.* **2008**, *43*, 5115.
[13] G. Zhang, M. Du, Q. Li, X. Li, J. Huang, X. Jiang, D. Sun, *RSC Adv.* **2013**, *3*, 1878.
[14] M. T. Klem, D. Willits, D. J. Solis, A. M. Belcher, M. Young, T. Douglas, *Adv. Funct. Mater.* **2005**, *15*, 1489.
[15] N. N. Kariuki, J. Luo, M. M. Maye, S. A. Hassan, T. Menard, R. Naslund, Y. Lin, C. Wang, M. H. Engelhard, C.-J. Zhong, *Langmuir* **2004**, *20*, 11240.
[16] Y. Yang, J. Shi, G. Kawamura, M. Nogami, *Scr. Mater.* **2008**, *58*, 862.
[17] J. E. Heuser, J. H. Keen, L. M. Amende, R. E. Lippoldt, K. Prasad, *J. Cell Biol.* **1987**, *105*, 1999.
[18] J. Heuser, T. Kirchhausen, *J. Ultrastruct. Res.* **1985**, *92*, 1.
[19] P. K. Sorger, R. A. Crowther, J. T. Finch, B. M. Pearse, *J. Cell Biol.* **1986**, *103*, 1213.
[20] T. Kirchhausen, *Annu. Rev. Biochem.* **2000**, *69*, 699.
[21] J. D. Wilbur, C.-Y. Chen, V. Manalo, P. K. Hwang, R. J. Fletterick, F. M. Brodsky, *J. Biol. Chem.* **2008**, *283*, 3287.
[22] C. Chih-Ying, F. M. Brodsky, *J. Biol. Chem.* **2005**, *280*, 6109.
[23] A. P. Schoen, D. T. Schoen, K. N. L. Huggins, M. A. Arunagirinathan, S. C. Heilshorn, *J. Am. Chem. Soc.* **2011**, *133*, 18202.
[24] L.-C. Cheng, J.-H. Huang, H. M. Chen, T.-C. Lai, K.-Y. Yang, R.-S. Liu, M. Hsiao, C.-H. Chen, L.-J. Her, D. P. Tsai, *J. Mater. Chem.* **2012**, *22*, 2244.
[25] S. Sadasivan, A. J. Patil, K. M. Bromley, P. G. R. Hastie, G. Banting, S. Mann, *Soft Matter* **2008**, *4*, 2054.
[26] J. R. Collette, R. J. Chi, D. R. Boettner, I. M. Fernandez-Golbano, R. Plemel, A. J. Merz, M. I. Geli, L. M. Traub, S. K. Lemmon, *Mol. Biol. Cell* **2009**, *20*, 3401.
[27] A. E. Miele, P. J. Watson, P. R. Evans, L. M. Traub, D. J. Owen, *Nat. Struct. Mol. Biol.* **2004**, *11*, 242.
[28] A. R. Ramjaun, P. S. McPherson, *J. Neurochem.* **1998**, *70*, 2369.
[29] A. Fotin, Y. Cheng, P. Sliz, N. Grigorieff, S. C. Harrison, T. Kirchhausen, T. Walz, *Nature* **2004**, *432*, 573.
[30] E. Ter Haar, S. C. Harrison, T. Kirchhausen, *Proc. Natl. Acad. Sci. U.S.A.* **2000**, *97*, 1096.
[31] S. Waelter, E. Scherzinger, R. Hasenbank, E. Nordhoff, R. Lurz, H. Goehler, C. Gauss, K. Sathasivam, G. P. Bates, H. Lehrach, E. E. Wanker, *Hum. Mol. Genet.* **2001**, *10*, 1807.
[32] J. A. Ybe, S. Mishra, S. Helms, *J. Mol. Biol.* **2007**, *367*, 8.
[33] J. M. Slocik, J. T. Moore, D. W. Wright, *Nano Lett.* **2002**, *2*, 169.
[34] R. R. Naik, S. J. Stronger, G. Agarwal, S. E. Jones, M. O. Stone, *Nat. Mater.* **2002**, *1*, 169.
[35] A. H. Pakiari, Z. Jamshidi, *J. Phys. Chem. A* **2007**, *111*, 4391.
[36] A. P. Schoen, K. N. L Huggins, S. C. Heilshorn, *J. Mater. Chem. B* **2013**, *1*, 6662.
[37] P. Alexandridis, *Chem. Eng. Technol.* **2011**, *34*, 15.
[38] A. P. Jackson, in *Methods in Molecular Biology, Biomembrane Protocols: I Isolation and Analysis*, (Eds: J. M. Graham, J. A. Higgins), Humana Press, Inc., Totowa, NJ **1993**, 83.
[39] J. Polte, X. Tuaev, M. Wuithschick, A. Fischer, A. F. Thuenemann, K. Rademann, R. Kraehnert, F. Emmerling, *ACS Nano* **2012**, *6*, 5791.
[40] C. A. Mirkin, T. A. Taton, R. L. Letsinger, *Science* **2000**, *289*, 1757.